Structure of a Low-Level Jet and it's Role in Triggering and Organizing Moist Convection over Taiwan: A TAMEX Case Study

BEN JONG-DAO JOU AND SHIUNG-MING DENG

ABSTRACT

This paper presents the kinematic and thermodynamic structure of a severe precipitating convective line associated with a low level jet (LLJ) observed during Taiwan Area Mesoscale EXperiment (TAMEX) on 24 – 25 June 1987. The meso- and convective-scale features of the Mei-Yu front and the associated quasi-stationary mesoscale convective systems that lead to heavy precipitation are described. The mesoscale structure of the LLJ and its relationship with the moist convection are emphasized.

The major convective precipitation associated with the convective line occurred at the pre-frontal region. At the post-frontal region, no organized reflectivity pattern existed. Accompanying the quasi-stationary convective line, a southwesterly LLJ of 20 ms^{-1} at 1 *km* existed. The LLJ decelerated when approaching the major convective precipitating areas and showed a distinct diffluent pattern. This flow structure produced concentrated, enhanced warm and moist air convergence which favored new convective cell formation. The strength of the deflection of the LLJ depends on the intensity of the convective downward motion associated with the mesoscale convective system.

1. INTRODUCTION

This paper presents the kinematic and thermodynamic structure of a vigorously precipitating convective line associated with a low level jet (LLJ) observed during Taiwan Area Mesoscale Experiment (TAMEX) on 24 – 25 June 1987. It is known from synoptic studies that during the China's Mei-Yu season and the Japan's Baiu season the occurrence of extremely heavy rainfall event has a close relationship with the presence of a LLJ in the 700 – 850 *mb* layer ahead of the surface front (Akiyama, 1973; Chen and Yu, 1988; Matsumoto, 1972; Ninomiya and Akiyama, 1974; Tao and Chen, 1987). However, the physical processes through which the LLJ and heavy precipitation are linked are not well understood. In early works, Matsumoto and Ninomiya (1971), Matsumoto (1972, 1973), Akiyama (1973), and Ninomiya and Akiyama (1974) suggested that the upward branch of the secondary circulation over the cyclonic shear side of the LLJ is responsible for the heavy

Department of Atmospheric Sciences, National Taiwan University, Taipei, Taiwan, R.O.C.

precipitation in Japan and the LLJ forms as a result of the cumulus-scale vertical exchange of horizontal momentum. By selecting 35 heavy rainfall events over Taiwan during Mei-Yu season, Chen and Yu (1988), on the other hand, suggested that the LLJ is the cause for the moist convection in Taiwan's Mei-Yu season. The main mechanism for the LLJ triggering the moist convection is through the creation of potential instability to the warm side of a Mei-Yu front and the generation of associated convergence downstream. They also suggested that vertical mixing by the cumulus convective process tends to dissipate rather than generate local LLJs.

In a two-dimensional frontogenesis model, Chou (1986) simulated the formation of a LLJ to the south of the area of strong convection. In his model, the LLJ formed through the Coriolis acceleration of the northward ageostrophic motion in the lower branch of the mesoscale secondary circulation induced by convective latent heat release. The mechanism may be interpreted as a mass-momentum adjustment process driven by diabatic heating and is supported by some observational and theoretical studies (Chen, 1982; Chen and Yu, 1988). In a recent modeling study, Nagata and Ogura (1991), using Japan Meteorological Agency (JMA)'s regional spectral model, suggested that the interaction between heavy precipitation and the LLJ is closely related to the associated diabatic heating processes. The super-geostrophic LLJ is formed under the situation where an air parcel crosses height contours into low pressure with large angles due to a combination of an alongfront flow in the southwestern portion of the anticyclonic outflow induced by the evaporating cooling and a crossfront flow in the upper part of the direct secondary circulation associated with the warm-frontogenetical processes.

In the above mentioned studies, works tend to focus on the effect of convective heating on the formation and maintenance of the LLJ in a synoptic and subsynoptic-scale framework. The role played by pre-existing LLJ in triggering and organizing the moist convection at meso- and smaller- scales is not discussed. Lemaitre and Brovelli (1990), using data from dual-Doppler radars, studied the kinematic and thermodynamic structure of a quasi-stationary convective line associated with a LLJ observed during LANDES-FRONTS 84. Their results suggested that in a strong baroclinic atmosphere, through symmetric instability and inertial acceleration, the transverse and vertical variations of the flow create slantwise motions on the left flank of the LLJ. The horizontal shear instability interacts with convective instability and is responsible for the organization of convection in that region. However, the meso- and small structure of LLJ was not clear demonstrated in their study and most conclusions were derived through indirect observational evidence.

This paper presents results of a dual-Doppler radar analysis for a case of heavy precipitation associated with a Mei-Yu front that occurred on 24 – 25 June 1987 over western Taiwan. The Mei-Yu front is characterized by a relatively weak baroclinic atmosphere but is accompanied by a strong moisture gradient and horizontal wind shear (Chen and Chang, 1980). The meso- and convective-scale features of the Mei-Yu front and the associated quasi-stationary convective line that leads to heavy precipitation are described. In the study, the mesoscale structure of a LLJ and its relationship with the moist convection are emphasized.

2. DATA AND ANALYSIS PROCEDURE

The data employed in the present study primarily originate from the multiple Doppler radar network operated during TAMEX period. NCAR CP4 Doppler radar and CAA (Civil Aeronautic Administration) Doppler radar data are combined to synthesize the horizontal wind fields for 7 consecutive volumes with time interval of 10 minutes (from 1720UTC to 1830UTC 24 June, 1740UTC data are missing).

In Figure 1, the small rectangle embedded in the big circle indicates the area (100 $km \times$ 70 km) of synthesized dual-Doppler horizontal winds. The grid distance is 1 km on both sides of the rectangle and 1 km in the vertical from 1 km to 15 km. The long axis of the rectangle rotates 35 degree counterclockwise from the east. The rotation of the domain is to make the long axis parallel to the major axis of the low level jet 1 km above the surface. In Figure 1, the position of surface cold front at 1800UTC 24 June, identified through detailed mesoscale surface analysis (Jou and Deng, 1990) is also marked. The surface front moved at a speed of 4 ms^{-1} toward the southeast and the convective line moved at approximately the same speed. The major convection (the blackened region denotes the echo pattern at 3 km height with reflectivity intensity larger than 40 dBZ) occurred in a region which is surrounded by the surface cold front, island topography, and the LLJ from the southwest. The convective line system has a spatial extent approximately 50 km wide and 200 km long. According to Jou and Deng (1990), new cells formed in the southwestern edge of the front then developed northeastward along the surface front. Mature cells existed at the northern part of the front and dissipated quickly as the cells approached to the coast or moved into the cold air region. The major convective precipitation associated with the convective line occurred in the pre-frontal region. This is quite different from that observed in midlatitude frontal rainbands and squall line systems (Hobbs and Persson, 1982; Carbone, 1982; Smull and Houze, 1987). At the cold side of the surface front, no organized reflectivity pattern existed. Accompanying with the quasi-stationary convective line, a LLJ from the southwest at 1 km height with the intensity of 20 ms^{-1} existed. It is the purpose of this study to show the structure of the LLJ and its role in triggering and organizing moist convection along the Mei-Yu front.

Data editing and processing were done with software developed in the Department of Atmospheric Sciences, NTU, which ported on a UNIX-based workstation. In order to test the reliability of the software, an inter-comparison between the results from NTU software and NCAR CEDRIC software has been conducted (Jou *et al.*, 1990). It was found that there is a good consistency between these two softwares. Nevertheless, the data recovery rate of CAA when using CEDRIC is relatively low in some low reflectivity regions. It was found in the CAA data pre-processing software, that whenever there existed a high wind variability region, data gaps occurred. Due to these problems, the effective resolution of the CAA data has been degraded. In order to resolve convective-scale features appropriately in this study, extremely careful data editing procedures (essentially, gate-by-gate) were performed to the CAA data. The time error check procedure proposed by Gal-Chen (1978) was also applied to minimize the possible errors existing in time differences of data sampling be-

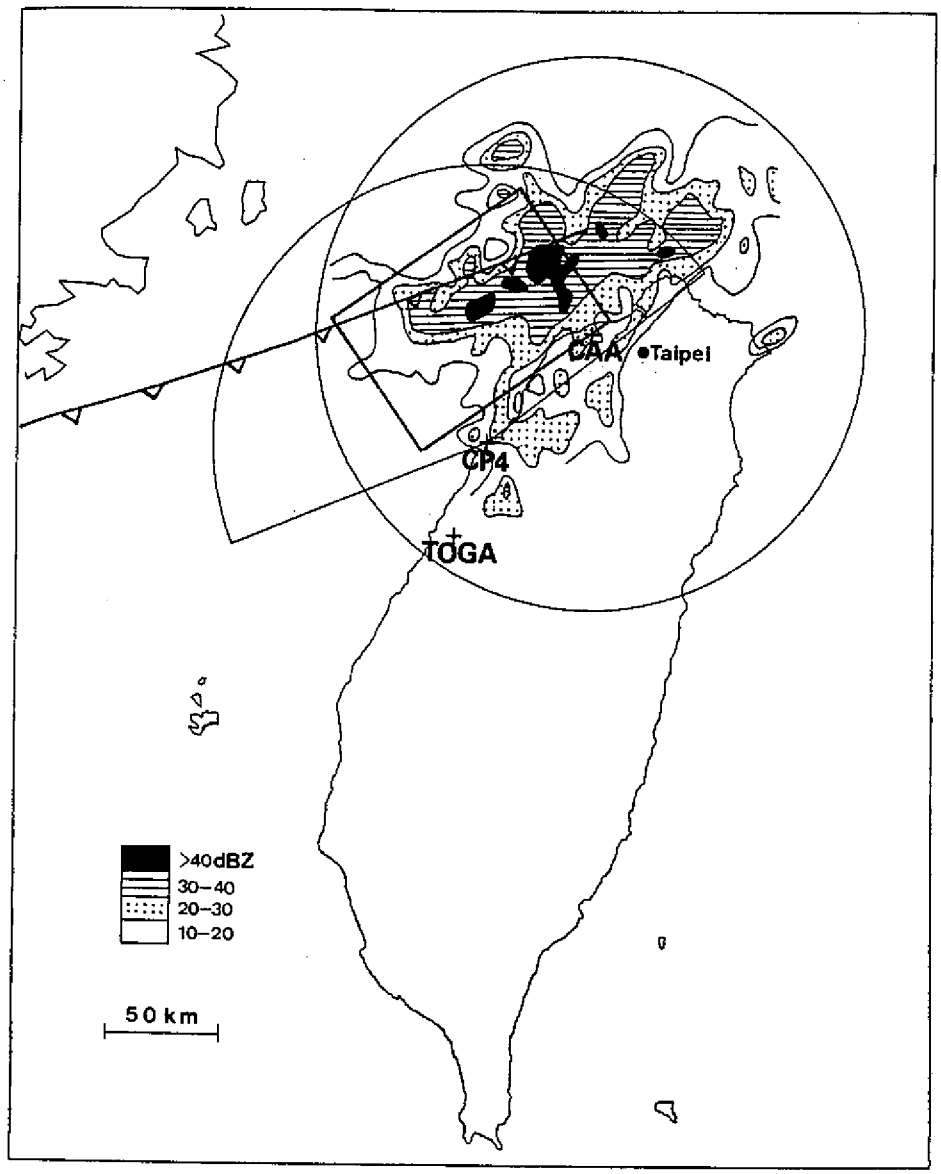

Fig. 1. Doppler radar network for TAMEX. The circles indicate the scanning strategies of CAA and CP4 during IOP13 (24 – 25 June, 1987). CAA radar was in a VAD mode with 12 elevation angles for each volume scan and CP4 radar was in a sector mode with 31 elevation angles. The small rectangle (100 *km* × 70 *km*) embedded in the circle is the area dual-Doppler synthesis was performed. The shaded region shows the reflectivity pattern at 3 *km* at 1800UTC 24 June. The position of the surface front at 1800UTC is also marked.

tween the two radars.

The data were analyzed with the dual-Doppler synthesis procedure described in Ray *et al.* (1980) and vertical velocity was calculated by using the variational method with anelastic equation as a dynamic constraint (Lin *et al.*, 1986).

3. RESULTS AND DISCUSSION

3.1 Environmental Conditions

Figures 2a and b show the skewT-logP plots of Taipei-PanChiao sounding on 1200UTC and 1800UTC 24 June. The sounding at 1200UTC represents the atmospheric conditions in the warm region ahead of the front and the sounding at 1800UTC represents the condition modified by the moist convection. The shading area in Figure 2a suggests that the atmosphere was potentially unstable with large CAPE. Above 600 *hPa*, the atmosphere was stable and dry. At low levels, there was a pronounced LLJ with a maximum intensity of 20 ms^{-1} at 1 *km* height (900 *hPa*). The winds veered with height above 950 *hPa* indicating warm-air advection associated with the LLJ. The sounding at 1800UTC (Figure 2b) showed a lapse rate close to moist adiabatic after modification by moist convection. However, a dry layer still existed in between 600 *hPa* to 400 *hPa*. The wind at near surface level was easterly and shifted to southwesterly at a higher altitude. The backing of the wind indicated a cold-air advection at the lower levels as the cold front moved through the region. At 1800UTC, the LLJ lifted to about 2 *km* with an intensity of 30 ms^{-1}. The lifting and intensification of the LLJ seems to have a close relationship with the moist convection associated with the frontal system.

3.2 LLJ at 1 *km*

Figures 3a–c show the dual-Doppler synthesized total horizontal winds (relative to the ground) at 1 *km* height on 1730, 1800, and 1830UTC 24 June. It should be noted that the streamlines are schematic and there is no intention to express the wind speed with the spacing of the adjacent streamlines. In these figures, the leading edge of the convergence zone (marked with a heavy solid line) is very close to the surface front. the flow structure away from the convergence zone is relatively simple. A rather uniform southwesterly flow with intensity of 18 – 21 ms^{-1} prevailed ahead (at the warm side of) the convergence zone. The jet core was located at the bottom (to the south) of the domain. The flow was almost parallel to the rotated x-axis with wind direction of 235 degree. Near the convergence zone, the jet speed decreased to 12 ms^{-1}. Pronounced horizontal shear existed on the cyclonic side of the LLJ. Behind the convergence zone (at the north side), the flow was from west (approximately 270 degree) with relatively weak speed. Strong shear convergence existed at the convergence zone. The flow structure is complicated near the strong convective region. The LLJ decelerated when approaching to a major convective precipitating area (denoted by I) and showed a diffluent pattern downwind. Associated with this diffluent flow pattern, a local wind maximum with extensive and concentrated momentum surge existed in a relatively small area ahead the convergence zone. This flow is suggested to have warm and moist characteristics.

In order to clearly show the above discussed phenomena, the dual-Doppler synthesized system-relative horizontal winds at 1 *km* height at 1730, 1800, and 1830UTC 24 June are given in Figures 4a–c. The difference between Figures 3 and 4 is that the moving speed of the convective line has been deducted and as such, the resultant winds are the flows relative

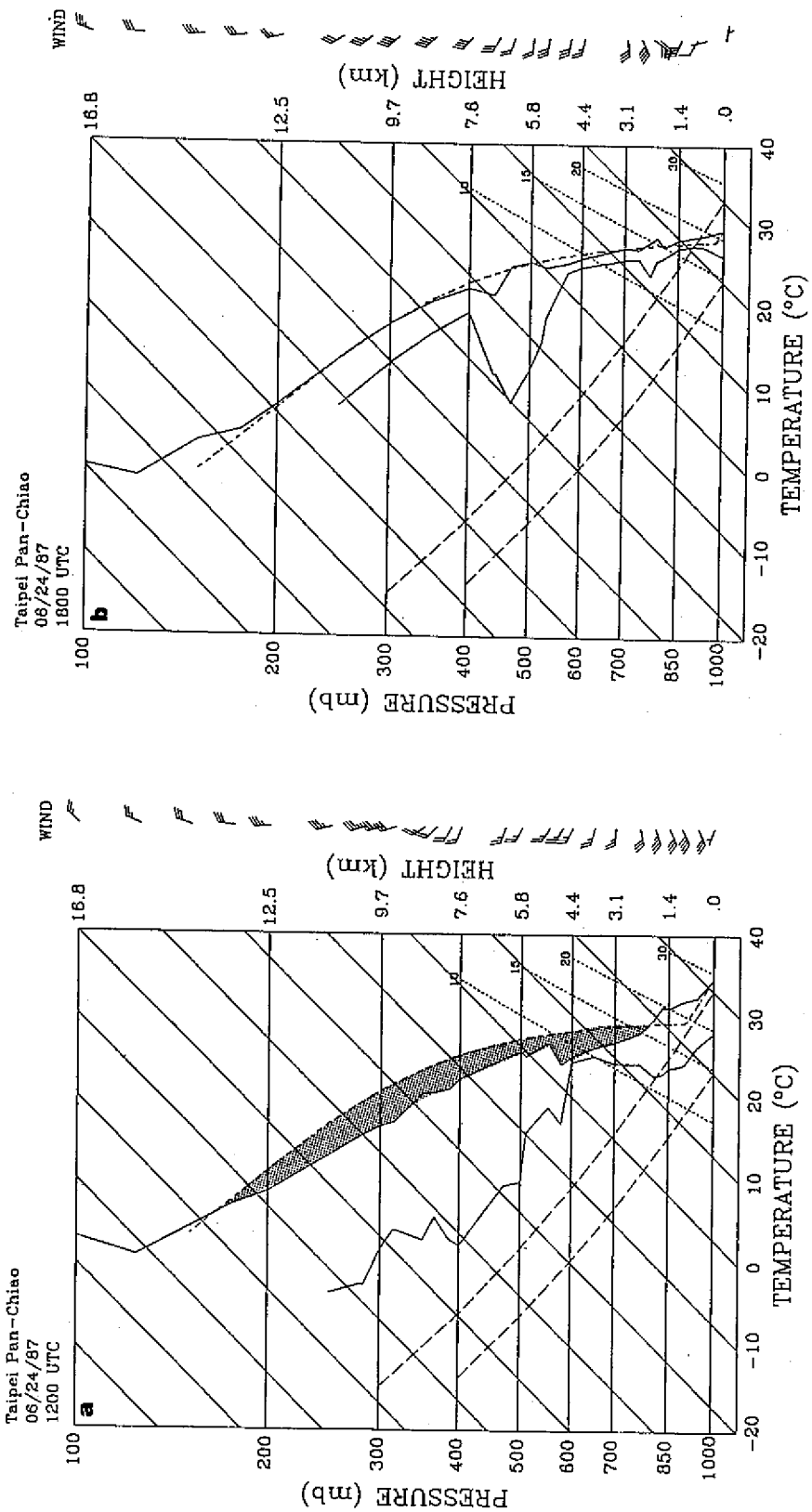

Fig.2. Soundings for Taipei Pan-Chiao station (46692), at (a) 1200UTC and (b) 1800UTC, 24 June 1987. Thermodynamic profiles plotted on skewT-logP diagrams, winds plotted at right, with full barb and half barb representing 5 and 2.5 ms^{-1}, respectively. Solid triangle in wind plot represents 25 ms^{-1}.

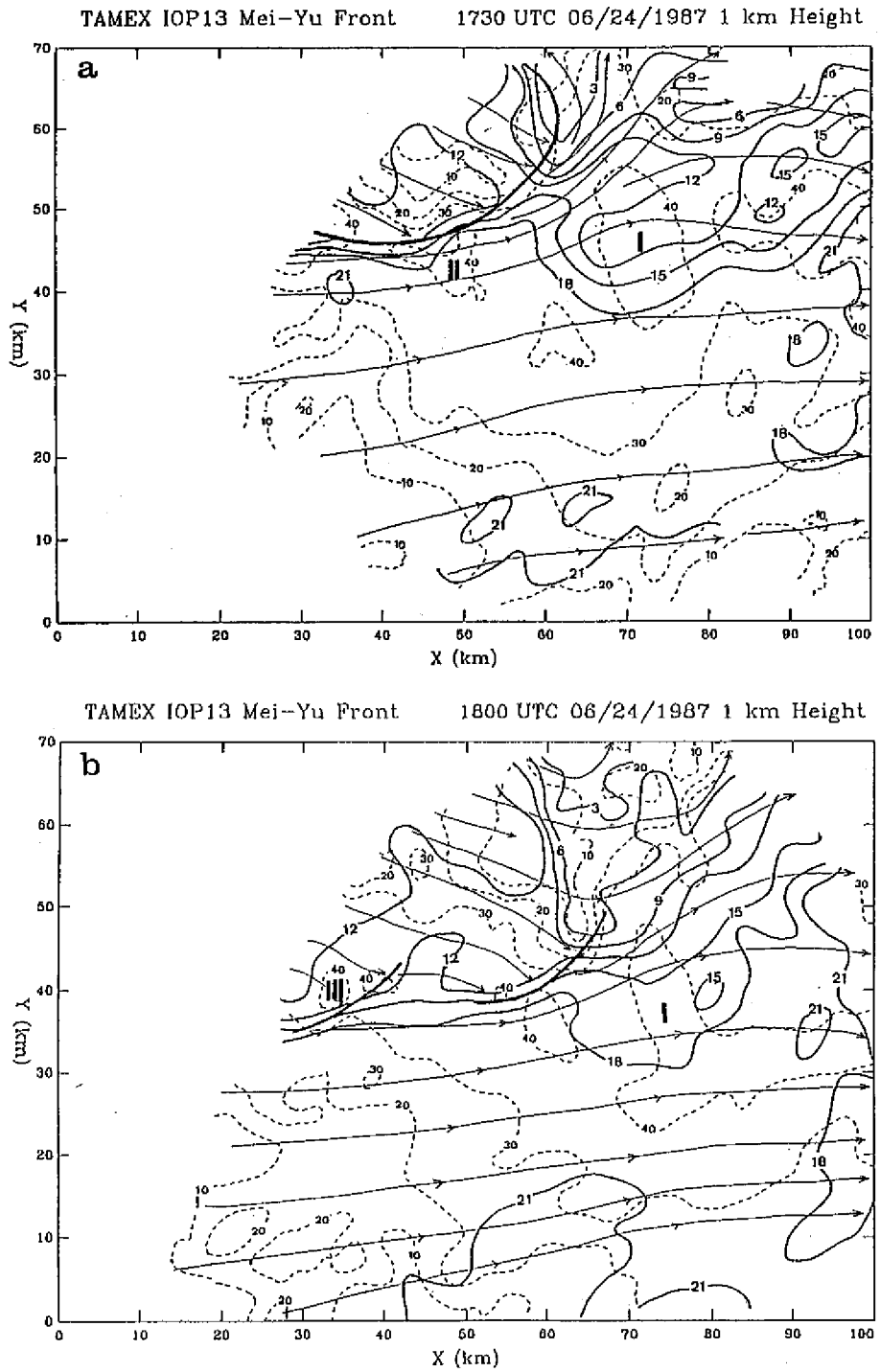

Fig. 3. Dual-Doppler synthesized total horizontal winds (relative to the ground) at 1 *km* height. (a) 1730UTC, (b) 1800UTC, and (c) 1830UTC, 24 June 1987. The thin-solid line represents the streamline, the solid line represents the isotach (ms^{-1}), and the thick-solid line represents the convergence zone. Reflectivity pattern at 1 *km* height is also shown (dash line) with contour interval of 10 *dBZ*.

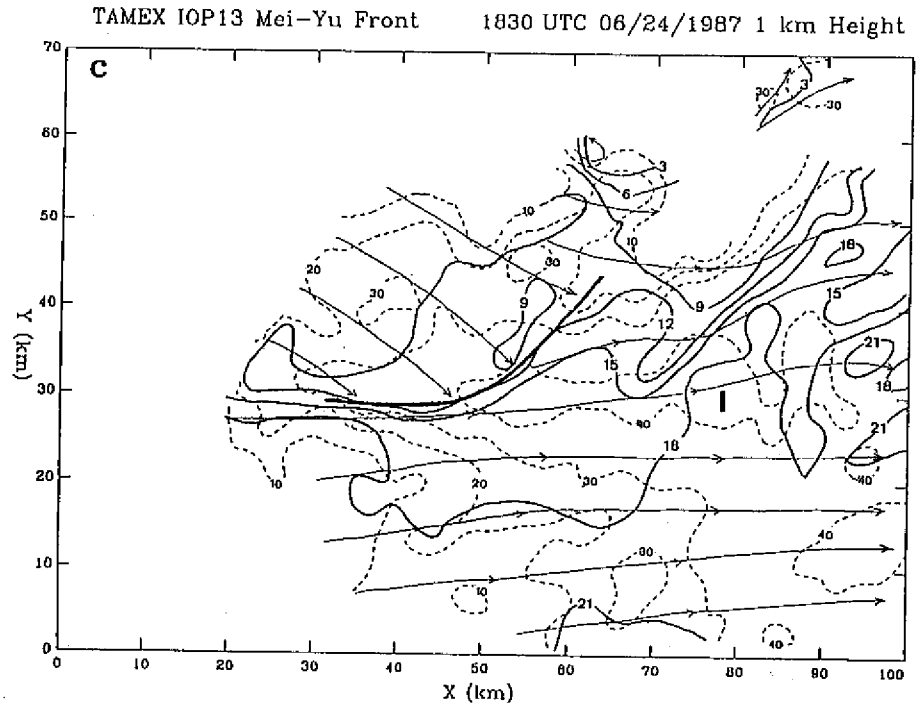

Fig. 3. Continued.

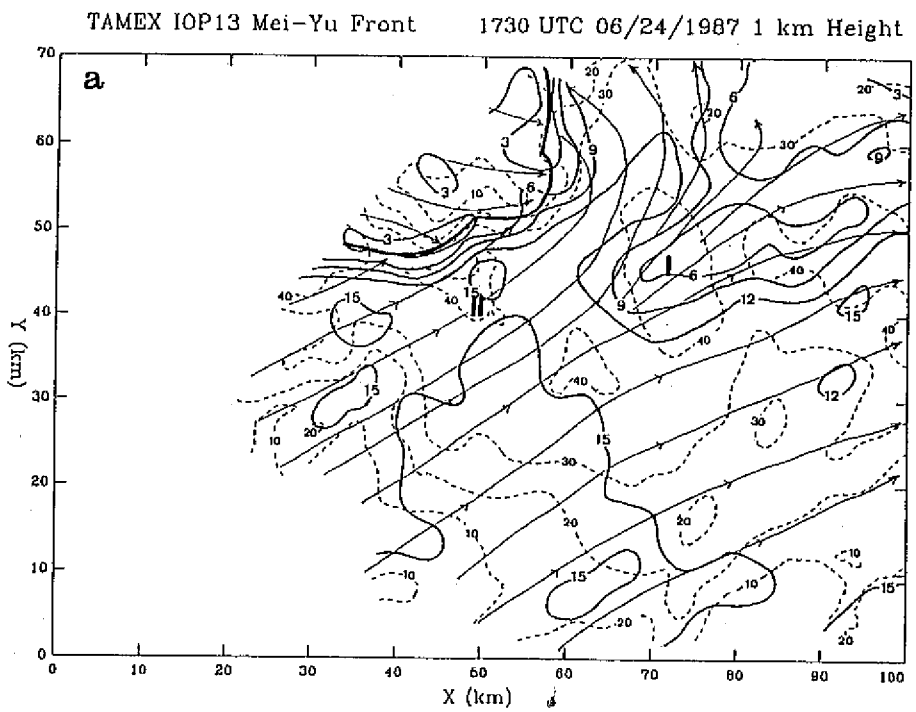

Fig. 4. The same as in Figure 3, but the horizontal winds are relative to the convective system. The moving speed of the system is 6.7 ms^{-1} in the x-axis and $-4.2\ ms^{-1}$ in the y-axis. The moving speed of the convective system is determined through calculating the correlation of reflectivity and wind velocity at consecutive times.

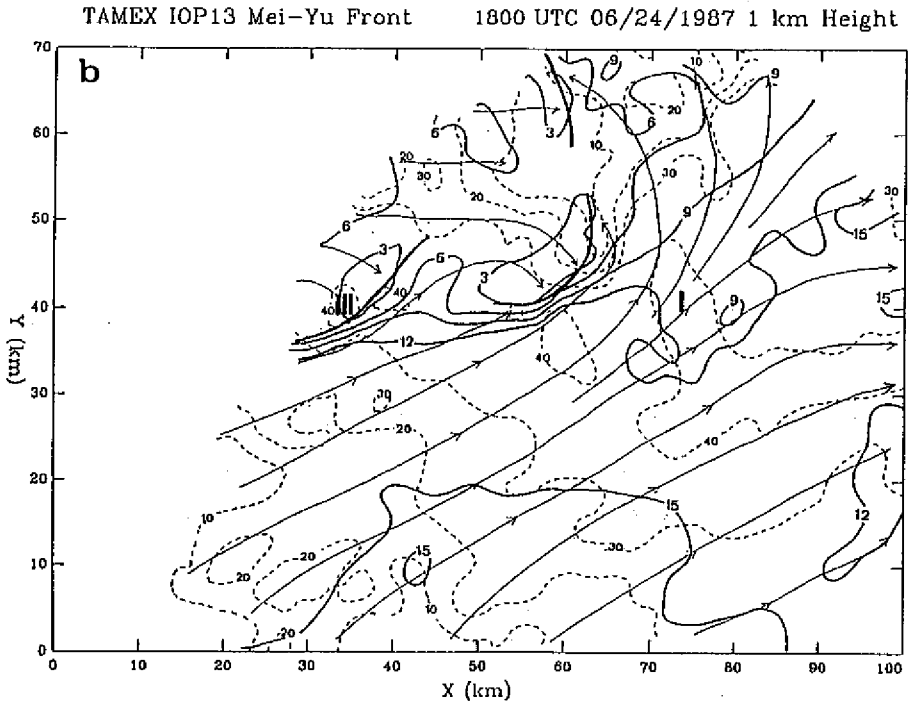

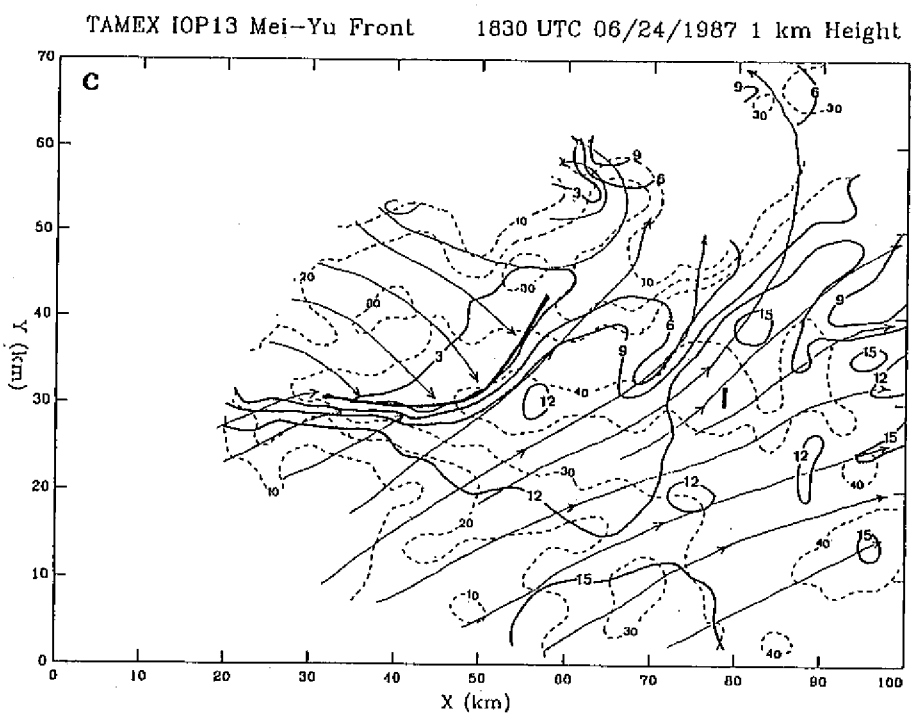

Fig. 4. Continued.

to the convective system. The results show that near the convective precipitating area I, the LLJ has experienced a large deflection. The cause of the deflection is possibly due to the horizontal perturbation pressure gradient induced by the convective downdraft associated with the heavy precipitation (see Figure 5 for the details of vertical motion distribution). The consequence of this flow structure is to produce a concentrated convergence area with warm and moist air surge which is favored for new cell formation. The sequences of this process can be seen from Figures 4a and 4b.

From a detailed examination of the time sequences of reflectivity data, convective systems II and III were quite short-lived with life time less than 30 minutes. Nevertheless, under almost the same environmental conditions, convective system I lasted for about 4 hours (started 1520 till 1900UTC). No satisfactory explanations are available now. However, it is speculated that the cyclonic circulation on the top of the domain of Figure 4c (1830UTC) might play an important role. The circulation was neither resolved in total horizontal wind plots (i.e., Figures 3a–c) nor in system-relative wind plots before 1830UTC. The results suggest there was possibly a separation of the pre-existing mesoscale cyclonic circulation and the convergence zone near 1830UTC. Before 1830UTC, the mesoscale cyclonic circulation and the convergence zone associated with the LLJ were geographically too close to be distinguished. The intensity of the convergence zone was possibly manifested due to the presence of the mesoscale cyclonic circulation. After the circulation separated away from the convergence zone, the long-lived convective system I dissipated quickly.

Formation of the mesoscale cyclonic circulation at the northwest corner of Taiwan has been studied by a numerical simulation experiment (Lin, 1990). His results showed that when the prevailing flow is northeasterly, a pronounced cyclonic circulation forms to the northwest of Taiwan. Accompanying with this cyclonic circulation, a mesoscale low pressure system is formed with the center located slightly to the west of the cyclonic circulation center. The existence of mesoscale low pressure system was also suggested subjectively over the approximately same location during IOP13 with TAMEX surface mesonet data by space-time conversion technique (Jou and Deng, 1990). Data over the water are needed before the details of this mesoscale circulation can be investigated.

3.3 Kinematic Structure on 1800UTC

a. Horizontal structure

The system-relative winds at 1800UTC 24 June 1987 are given in Figure 5. At 1 *km* (Figure 5a), the shaded regions show the vertical component of relative vorticity field. Above 1 *km* (Figures 5b–f), the light shaded regions show the convective updrafts and the heavy shaded regions show the convective downdrafts. The solid contours show the reflectivity field. Some prominent features are summarized below.

The LLJ existed at and below 3 *km*. For regions away from convections, the maximum wind speed was at 1 *km* height. On the other hand, the maximum wind speed was at a higher altitude (approximately 2 *km*) where moist convection presented. The cyclonic shear side of

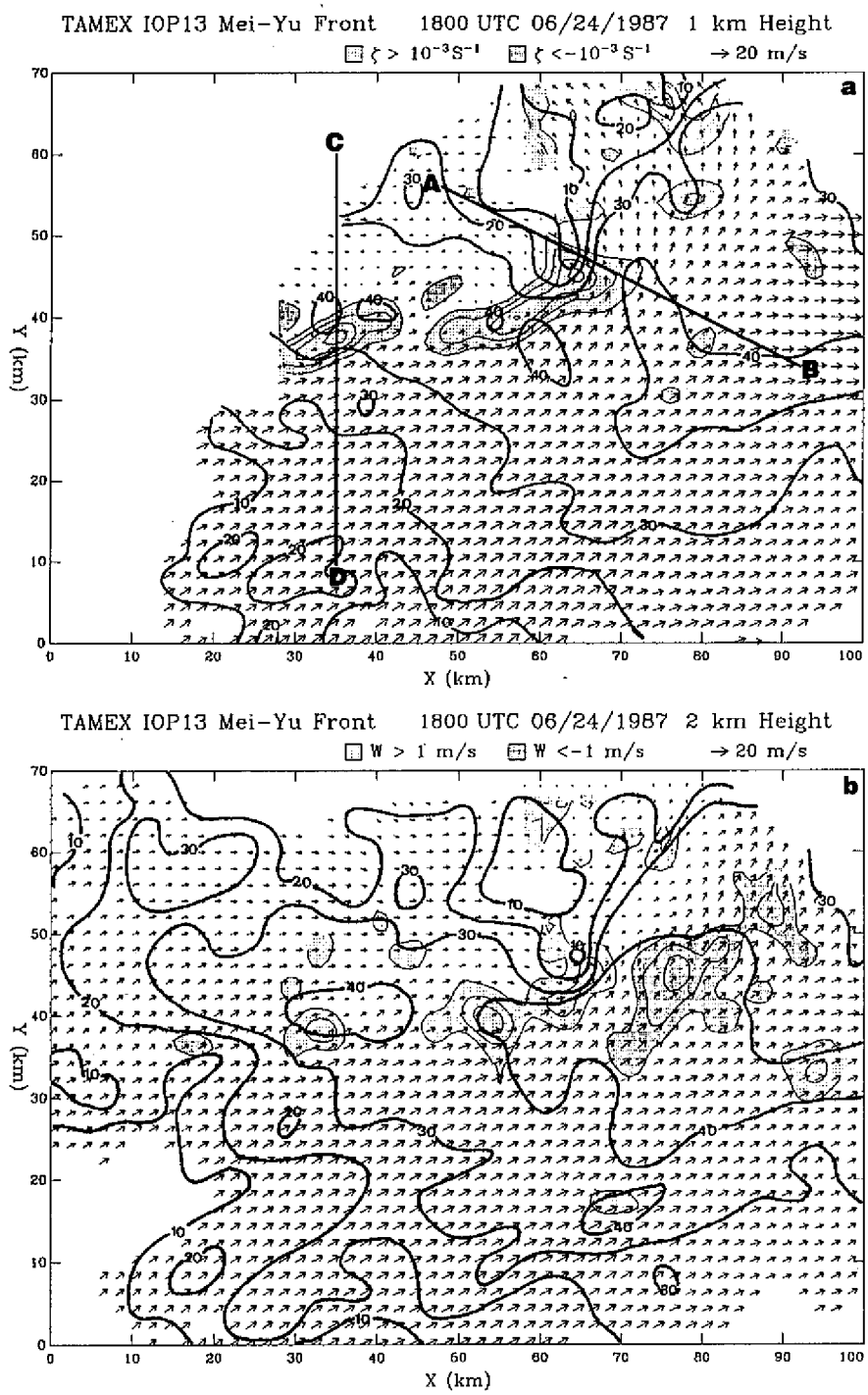

Fig. 5. The system-relative winds at 1800UTC 24 June 1987. The thick-solid line encloses reflectivity with contour interval of 10 *dBZ*. At 1 *km* plot, the shading represents the vertical component of vorticity larger than $1.0 \times 10^{-3} s^{-1}$ (light) or less than $-1.0 \times 10^{-3} s^{-1}$ (heavy), respectively. The solid lines A-B and C-D represent the vertical cross sections chosen for discussion. At other levels, the light shading represents updraft larger than 1 ms^{-1} and the heavy shading represents downdraft less than -1 ms^{-1} with same contour interval of 1 ms^{-1}.

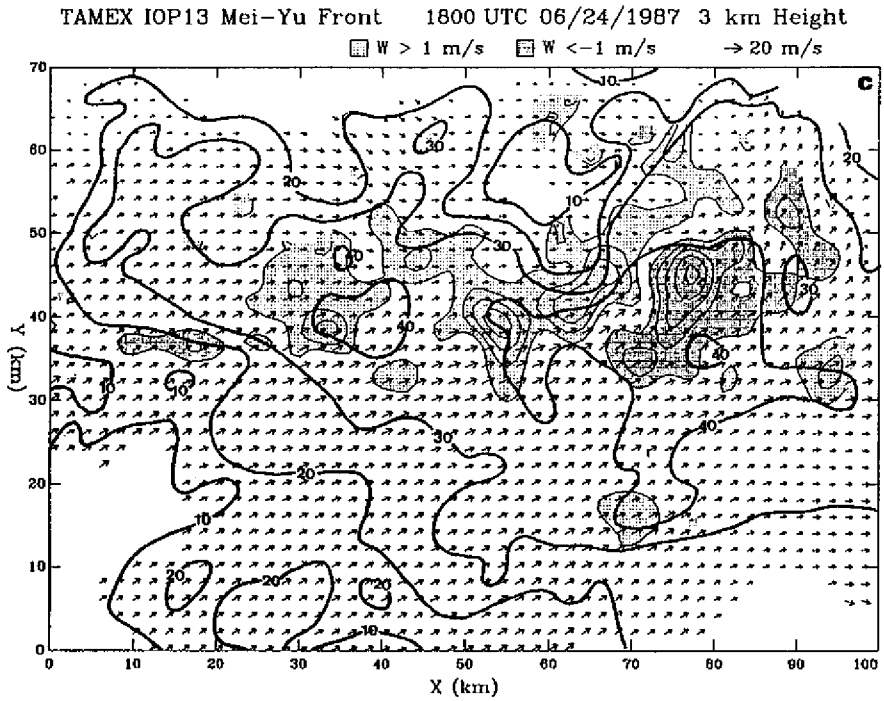

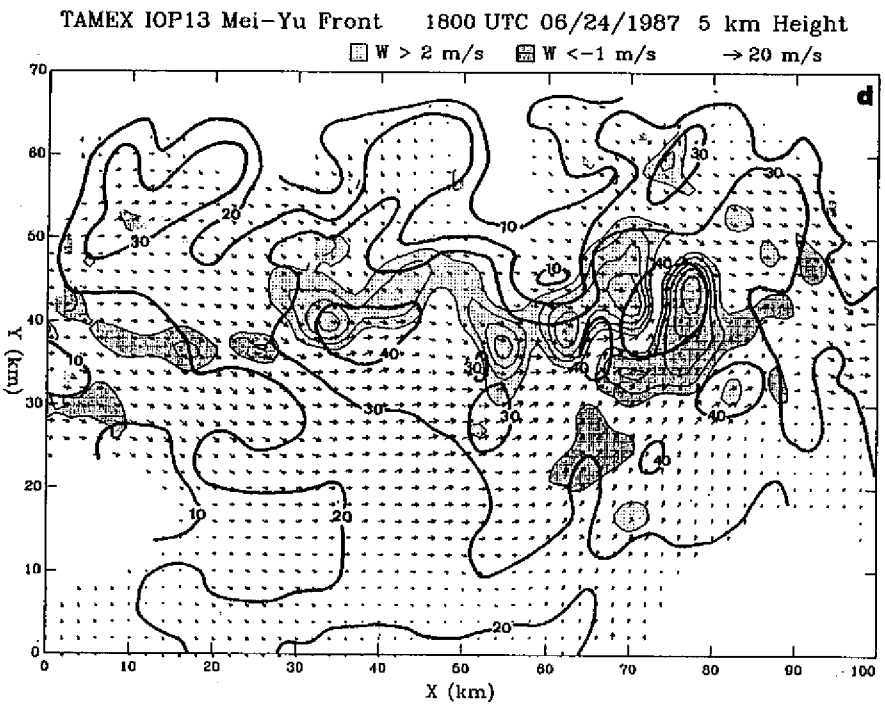

Fig. 5. Continued.

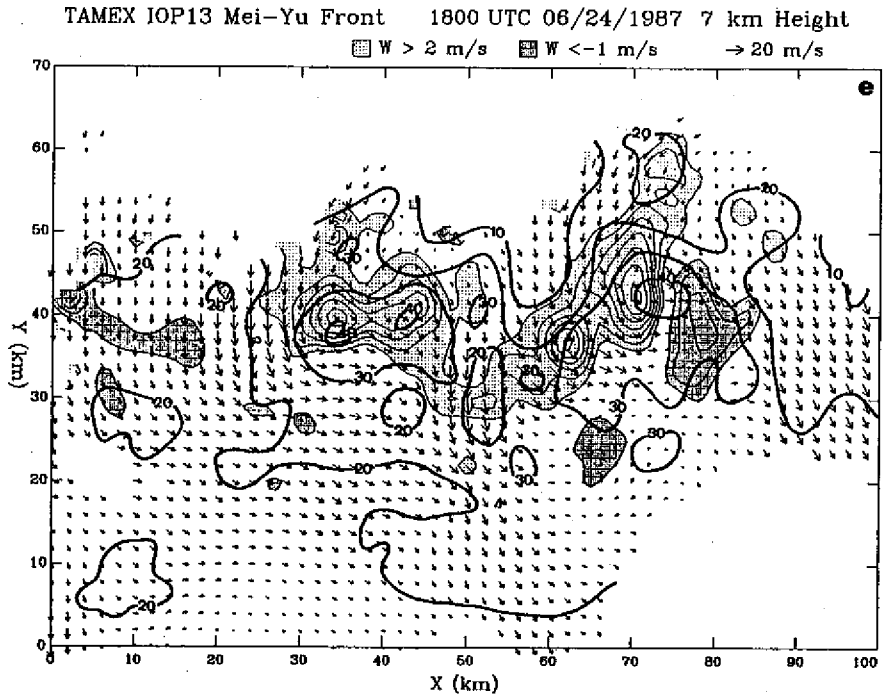

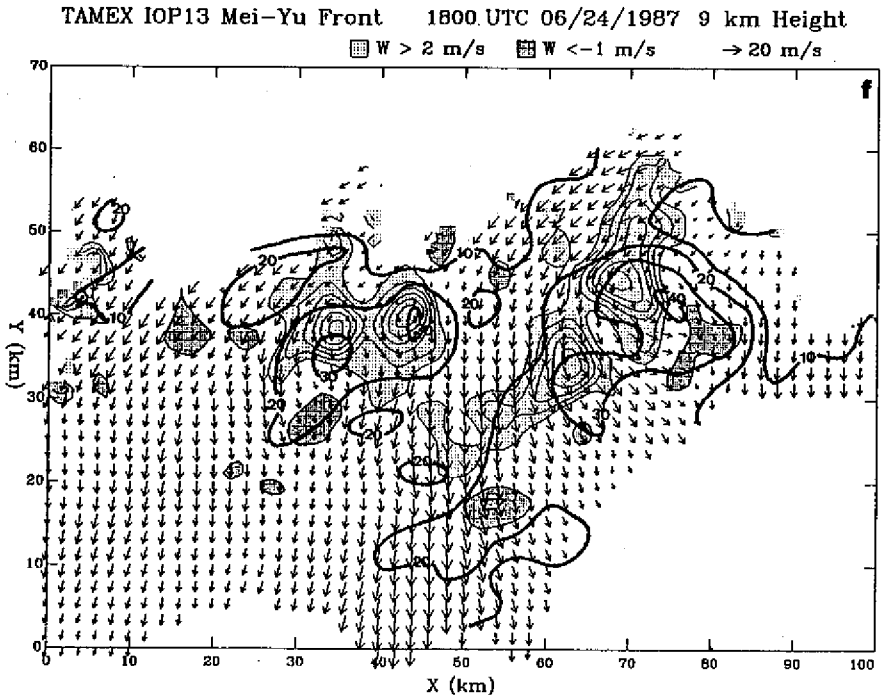

Fig. 5. Continued.

LLJ is accompanied with large positive vorticity and its maximum amplitude reached 5.0×10^{-3} s^{-1} at 1 *km*. The vorticity field has an elongated structure and was colocated with the convergence zone as shown in Figure 3. The low-level ascending motion was also colocated with the positive vorticity field. Relative to low-level positive vorticity field, the upward motion at and above 5 *km* showed a tilt to the warm side of the convergence zone. The upward motion and the vorticity fields at low levels both showed pronounced wave-like periodic features with a wavelength of approximately 8 *km*. It is noted that the wave-like structure of low-level convergence is 180 degree out of phase with the low-level vorticity field. The result suggests that tilting, rather than stretching, is the primary production mechanism. The maximum upward motion occurred at 7 – 9 *km* with amplitude of 11 ms^{-1}.

Organized descending motion was observed at the warm side of low-level convergence zone. The maximum downward motion occurred at about 4 – 5 *km* height with amplitude of 7 ms^{-1}. The amplitude of the descending motion is rather large compared with that observed from oceanic convection over Taiwan area (Jorgensen and LeMone, 1989). The subsidence area associated well with the reflectivity pattern at low levels and was probably driven by water loading.

On the top of the domain, there was a bounded weak echo region at the cold side of the convergence zone. The weak echo region existed at all levels, however, bounded only at levels below 5 *km*. Associated with the weak echoes, a relatively weak descending motion (< -1 ms^{-1}) existed at high levels. As pointed out earlier, this region was accompanying a mesoscale cyclonic circulation at the planetary boundary layer. The results suggest this mesoscale cyclonic circulation was possibly a warm core low pressure system.

The structure of upward and downward motions shown in Figure 5 suggests the convective cells associated with the convective line were going through different stages of their life time. New cells developed at southwestern edge of the front then propagated northeastward to its mature stage. The results also suggest the low-level flows were distorted to different degrees according to the strength and stage of the convective activity. LLJ exhibited a large deflection component toward the cyclonic side when convective downward motion of large spatial extent were encountered. The deflection was largest at low levels. The deflection of LLJ produced a local concentrated region with enhanced convergence, consequently, induced an area with enhanced convective activity. If this sequence were to continue, the enhanced convection would again strengthen the intensity of the convective downward motion and further change LLJ structure. This is a possible physical mechanism with positive feedback processes to maintain and organize moist convections along Mei-Yu front in TAMEX IOP13.

b. Vertical structure

Figure 6 show the vertical cross sections of system-relative winds and reflectivity along lines A-B and C-D given in Figure 5. Line A-B is chosen to show the flow structure of a mature convective cell (marked with I in Figure 3) in a vertical plan perpendicular to the LLJ, and line C-D is chosen to show the flow structure of a developing convective system

(marked with III in Figure 3) on the southwestern edge of the Mei-Yu front. The cross section of C-D has a smaller angle with the direction of LLJ, thus, the flow parallel to the plane presents most of the characteristics of the LLJ at the warm side of the front.

(1) Cross section C-D

The reflectivity pattern of C-D (Figure 6a) showed a narrow large echo region (> 40 *dBZ*) reaching a height of 6 *km*. Precipitation echoes at upper levels leaned forward over the inflow region. The high reflectivities correlated well with the ascending motion at low levels. The maximum updraft associated with the convective system had an amplitude larger than 9 ms^{-1} located at 7 – 9 *km*. The updraft tilted backward at low levels and tilted

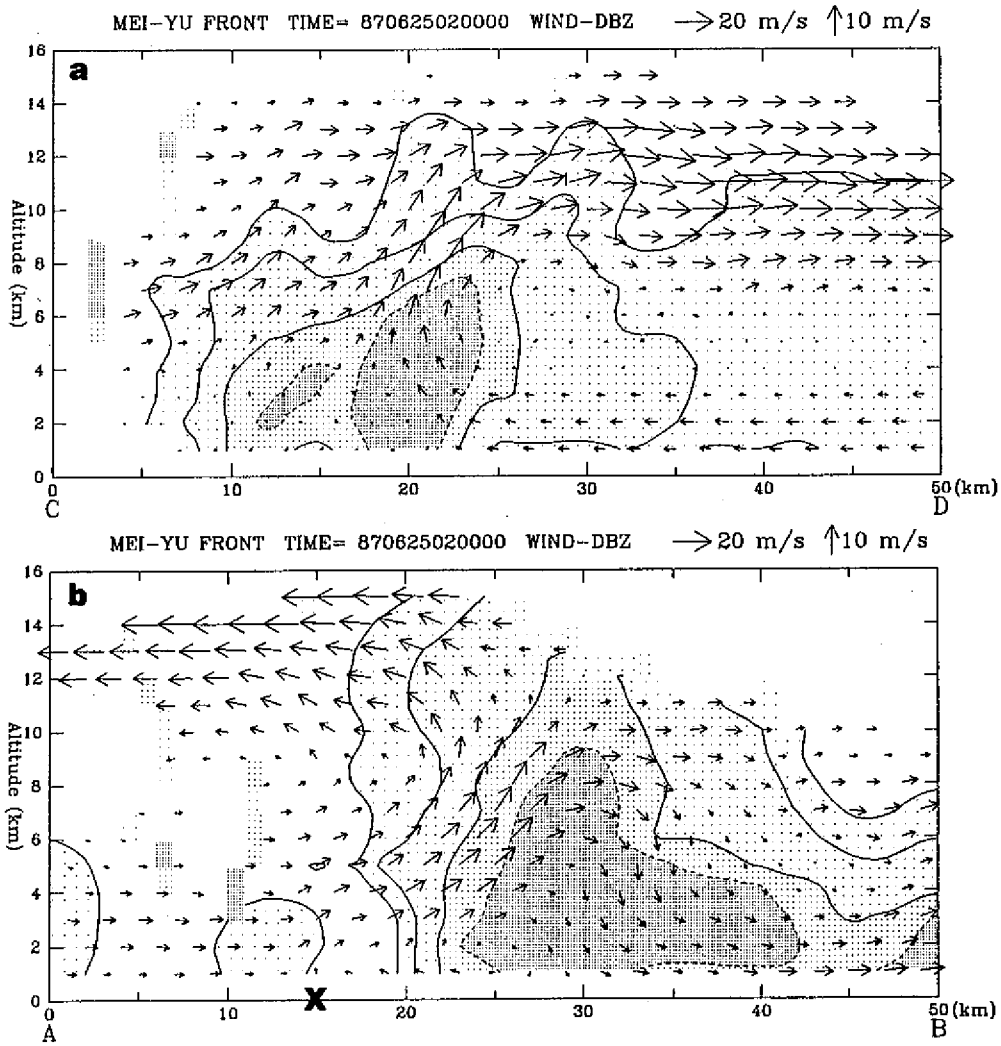

Fig. 6. Vertical cross-sections of wind and reflectivity along lines A-B and C-D shown in Figure 5. The minimum contour of reflectivity is 15 *dBZ* and contour interval is 10 *dBZ*. The heavy shading represents reflectivity larger than 40 *dBZ*.

forward above 5 *km*. There was an indication of upper-level downward motion at 8 *km* height ahead of the updraft with an amplitude less than 2 ms^{-1} and spatial extent smaller than 5 *km*.

Low-level winds ahead of the convection entered the system below 4 *km*. Large low-level convergence forced upward motion at the front of the major convective precipitating area. The ascending motion tilted backward due to the penetration of the low-level winds ahead the convection. It is noted that low-level winds at the rear of the convection were from the north and rather weak. However, a relatively strong low-level northerly winds existed at 1 *km* height and extended forward to the boundary of the inflow region. Large convergence occurred at the boundary where these two flows met. There was no convective downward motions associated with this shallow, extended forward northerly flows and this was not a gust front-type flow caused by convective outflow boundary. We believe that this is an indication of the post-frontal cold air flows accompanied with the surface Mei-Yu front. The flow structure suggests the cold air at the rear of the Mei-Yu front has a depth about 1 *km* height and has a sharp boundary corresponding to the warm air flow ahead of the front.

Upper-level winds were relatively simple. The flows were from the north. At 7 *km* there was a relatively strong inflow from rear of the convection. Due to the flow structure at upper levels, the precipitation echoes leaned forward to pre-frontal regions.

(2) Cross section A-B

The reflectivity pattern of A-B (Fig.6b) showed large echoes (> 40 *dBZ*) extended to a large area. Besides the convective precipitating region at the forefront of the convective ascending motions, there existed a forward extension of large echoes at low-levels. The size of the large-echo area was at least larger than 30 *km* in one dimension. The major convective ascending motions were not colocated with the maximum reflectivity area as shown in section C-D. The major convective upward motions located 5 – 10 *km* west (to the left) of the major reflectivity and tilted forward. The convective downward motions existed in the pre-frontal region and were colocated with the forward extension of large echoes. The maximum intensity of the convective downdraft occurred at 4 – 6 *km* height with amplitude larger than 7 ms^{-1}.

The low-level winds in the pre-frontal region blew away from the convective region, exhibiting the signature of convective outflows. At the first glance, the cross section suggests the inflows were from the "back" of the convective system. Since the plan is almost perpendicular to the direction of LLJ, the signature of the LLJ are not exhibited. However, if we examine carefully, we can see that at bottom of the plot (1 *km* height) at 15 – 25 *km* position, there was a flow from the pre-frontal region (front-to-rear). The flow from the pre-frontal region met the flow from post-frontal region at a position marked by a "X" (15 *km* from the left boundary). Notice that the position of X is at the rear echo boundary of the convective precipitating system. The position X possessed the maximum low-level convergence and induced a low-level convective upward motion. This flow structure is quite different from that obtained from cross section C-D. In C-D, the low-level convergence and upward motions were at forefront of the convective system. In A-B, the low-level conver-

gence and upward motions occurred at the rear boundary of the convective system.

In Figure 7, the speed of the flow perpendicular to the plan of A-B is shown. Positive value represents winds flow into the paper (i.e., approximately, to the north). It is noted that the low-level inflow region (15 – 25 *km*) was associated with the largest cyclonic shear of the LLJ. The region also accompanied the largest low-level convergence (Figure 6b). Convective activities were maintained and organized where the pronounced low-level convergence prevailed. Thus, the triggering and organizing the moist convections along the Mei-Yu front is closely related to the structure of the LLJ and the induced convective motions.

In Figure 7, it is also important to point out that the flows from the south (into the paper) at pre-frontal region reach 9 *km* height, however, from C-D cross section (see Figure 6a), the flows from the south (to the left of the domain) was only limited to altitudes below 4 *km*. This figure provides an observational evidence that the southerly momentum of a low-level jet could be transported to higher altitudes through organized moist convective activities.

The flow structure of A-B cross section exhibits some very interesting messages. Firstly, the low-level inflows of the system were from the third dimension (into the paper) which was the direction of the LLJ. Thus, in order to clearly exhibit the flow structure associated with the convective system, a three-dimensional description is necessary. Secondly, since the flow structure was three-dimensional, the pre-frontal heavy precipitation was not necessary to be a factor to cease the convective activity due to the inflow contamination. In fact, we believe that the presence of the pre-frontal convective downward motions associated with the convective precipitation exerted a force to deflect the LLJ when the jet passed by the region between the heavy precipitation and the low-level convergence zone. This effect is to enhance local convective activity instead to cease it.

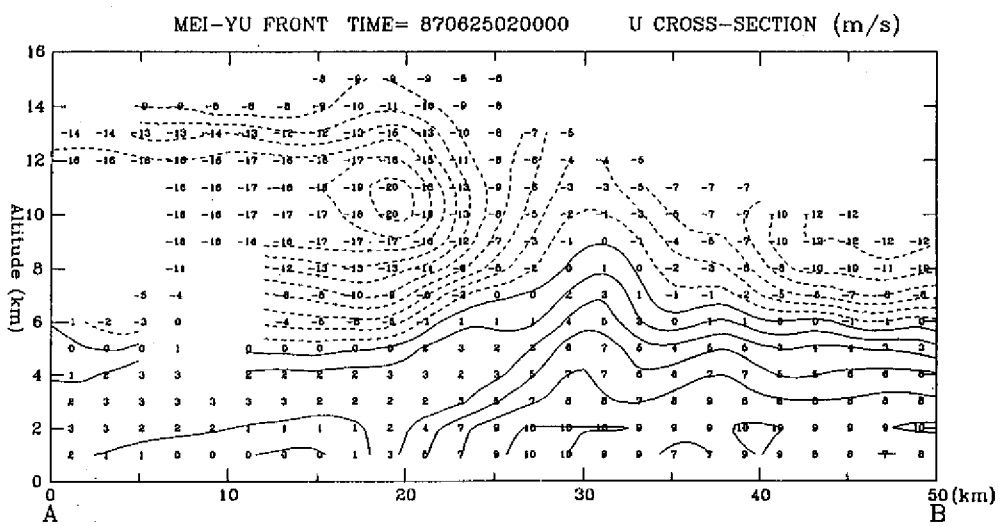

Fig. 7. Vertical cross-section of winds perpendicular to the line A-B shown in Figure 5.

4. CONCLUSIONS

A dual-Doppler radar analysis for a case of heavy precipitation associated with a Mei-Yu front occurred on 24 – 25 June 1987 over western Taiwan is presented in this paper. The mesoscale structure of a LLJ and its relationship in triggering and organizing moist convection are emphasized. Some preliminary conclusions are:

(1) The enhanced and concentrated convergence on the cyclonic side of the LLJ is the main factor to trigger moist convections along the convergence zone.

(2) The organization of moist convections is closely related to the structure of the LLJ, the upper-level flows, and the thermodynamic property of the atmosphere.

(3) The deflection of LLJ by organized pre-frontal convective downward motion produces a local concentrated region with enhanced convergence of momentum, heat, and moisture along the front. The concentrated convergence will induce enhanced convective activity at that region. If this sequence were continued, the enhanced moist convection would again strengthen the intensity of the convective downward motion and then change LLJ structure. This is the possible physical mechanism with positive feedback processes to maintain and organize moist convection along Mei-Yu front in TAMEX IOP13.

Acknowledgements This research is supported in part by NSC80-0202-M002-27. Discussions with Professor Richard Johnson are highly appreciated.

REFERENCES

Akiyama, T., 1973: Frequent occurrence of the heavy rainfalls along the north side of the low-level jet stream. *Pap. Meteor. Geophys.*, **24**, 379-388.

Carbone, R.E., 1982: A severe frontal rainband. Part I: Stormwide hydrodynamic structure. *J. Atmos. Sci.*, **39**, 258-279.

Chen, G.T.J., and C.P. Chang, 1980: The structure and vorticity budget of an early summer monsoon trough (Mei-Yu) over southeastern China and Japan. *Mon. Wea. Rev.*, **108**, 942-953.

Chen, G.T.J., and C.C. Yu, 1988: Study of low-level jet and extremely heavy rainfall over northern Taiwan in the Mei-Yu season. *Mon. Wea. Rev.*, **116**, 884-891.

Chen, Q., 1982: The Instability of the gravity-inertia wave and its relation to low-level jet and heavy rainfall. *J. Meteorol. Soc. Jpn.*, **60**, 1041-1057.

Chou, L.C., 1986: A numerical simulation of the Mei-Yu front and the associated low-level jet. *Ph.D. thesis, Naval Postgraduate School*, 157 pages.

Gal-Chen, T., 1978: A method for the initialization of the anelastic equations: Implications for matching methods with observations. *Mon. Wea. Rev.*, **106**, 587-606.

Hobbs, P.V., and P.O.G. Persson, 1982: The mesoscale and microscale structure and organization of clouds and precipitation in mid-latitude cyclones. Part V: The substructure of narrow cold-frontal rainbands. *J. Atmos. Sci.*, **39**, 280-295.

Jorgensen, D.P., and M.A. LeMone, 1989: Vertical velocity characteristics of oceanic convection. *J. Atmos. Sci.*, **46**, 621-640.

Jorgensen, D.P., M.A. LeMone, and B.J.-D. Jou, 1991: Precipitation and kinematic structure of an oceanic mesoscale convective system. Part I: Convective line structure. *Mon. Wea. Rev.*, **119**, 2608-2637.

Jou, B.J.-D., and S.M. Deng, 1990: Mesoscale characteristics of Mei-Yu front. A TAMEX case study. *Proc. Workshop on TAMEX Scien. Results, Sept.* 24-26, *Boulder, CO.*, 150-157.

Jou, B.J.-D., J.S. Hong, and S.M. Deng, 1990: Dual-Doppler radar analysis of a convective (Mei-Yu) frontal rainband. *Atmos. Sci.*, **18**, **3**, 239-264. (In Chinese with English abstract)

Lemaitre, Y., and P. Brovelli, 1990: Role of a low-level jet in triggering and organizing moist convection in a baroclinic atmosphere. A case study: 18 May 1984. *J. Atmos. Sci.*, **47**, 82-100.

Lin, Y.J., T.C. Wang, and J.H. Lin, 1986: Pressure and temperature perturbations with a squall-line thunderstorm derived from SESAME dual-Doppler data. *J.Atmos. Sci.*, **43**, 2302-2327.

Lin, Y.L., 1990: Formation mechanisms of Taiwan mesolows during the Mei-Yu season. *Proc. Workshop on TAMEX Scien. Results*, Sept. 24-26, *Boulder, CO*, 174-181.

Matsumoto, S., 1972: Unbalanced low-level jet and solenoidal circulation associated with heavy rainfalls. *J. Meteorol. Soc. Jpn.*, **50**, 194-203.

Matsumoto, S., 1973: Lower tropospheric wind speed and precipitation activity. *J. Meteor. Soc. Jpn.*, **51**, 101-107.

Matsumoto, S., and K. Ninomiya, 1971: On the mesoscale and medium-scale structure of a cold front and the relevant vertical circulation. *J. Meteorl. Soc. Jpn.*, **49**, 648-662.

Nagata, M., and Y. Ogura, 1991: A modeling case study of interaction between heavy precipitation and a low-level jet over Japan in the Baiu season. *Mon. Wea. Rev.*, **119**, 1309-1336.

Ninomiya, K., and T. Akiyama, 1974: Band structure of mesoscale clusters associated with low-level jet stream. *J. Meteorol. Soc. Jpn.*, **52**, 300-313.

Ray, P., C. Ziegler, W. Bumgarner, and R. Serafin, 1980: Single and multiple Doppler radar observations of tornadic storms. *Mon. Wea. Rev.*, **108**, 1607-1625.

Smull, B.F., and R.A. Houze, Jr., 1987: Dual Doppler radar analysis of a midlatitude squall line with a trailing region of stratiform rain. *J.Atmos. Sci.*, **44**, 2128-2148.

Tao, S., and L. Chen, 1987: A review of recent research on the East Asian summer monsoon in China. *Monsoon Meteorology, C.P. Chang and T.N. Krishnamurti, EDs., Oxford University Press*, 60-92.

低層噴流的結構及其在激發與組織台灣區濕對流之角色：TAMEX個案研究

周仲島　鄧秀明
國立台灣大學大氣科學研究所

摘　要

本文係討論在 TAMEX 實驗期間，1987 年 6 月 24～25 日在台灣西北部外海地區伴隨低層噴流之劇烈鋒面雨帶的運動場結構。文中除了描述此鋒面雨帶的中尺度與對流尺度運動場結構外，並特別說明低對流層（1 公里高度低層噴流在劇烈對流區）水平結構。

結果顯示此鋒面雨帶的主要對流降水在鋒前暖區，鋒後並無明顯層狀降水區，此與中緯度及熱帶颮線系統的中尺度回波結構頗爲不同。鋒前 1 公里高度有明顯西南低層噴流，風速可達 20 公尺/秒。此低層西南氣流在接近鋒前對流降水區時明顯減弱，且呈偏轉。低層噴流之偏轉與鋒前伴隨對流降水之對流尺度下沖流強度成正比。對流尺度下沖流所在位置在近地層將伴隨一中尺度高壓，此中尺度高壓與鋒面區之水平氣壓梯度將加強，使得低層噴流垂直鋒面之分量得以被加強。